BULLETIN OF THE POLISH ACADEMY OF SCIENCES
TECHNICAL SCIENCES
Vol. 54, No. 2, 2006

BN-based nano-composites obtained by pulsed laser deposition

B. MAJOR[1]*, W. MRÓZ[2], M. JELINEK[3], R. KOSYDAR[1], M. KOT[4], Ł. MAJOR[1], S. BURDYŃSKA[2], and R. KUSTOSZ[5]

[1]Institute of Metallurgy and Materials Science, Polish Academy of Sciences, 30-059 Cracow, 25 Reymonta St., Poland
[2]Institute of Optoelectronics, Military University of Technology, 01-483 Warsaw, 2 Kaliski St., Poland
[3]Institute of Physics, Academy of Science of the Czech Republic, Prague 8, Na Slovance 2, Czech Republic
[4]Tribology and Surface Engineering Laboratory, AGH University of Science and Technology, 30 Mickiewicza Ave, 30-059 Cracow, Poland
[5]Foundation of Cardiac Surgery Development, 345a Wolnosci St., 41-800 Zabrze, Poland

Abstract. Boron nitride thin layers were produced by means of the pulsed laser deposition technique from hexagonal boron nitride target. Two types of laser i.e. Nd:YAG with Q-switch as well as KrF coupled with RF generator were used. Influence of deposition parameters on surface morphology, phase composition as well as mechanical properties is discussed. Results obtained using Fourier Transformed Infrared Spectroscopy, Transmission and Scanning Electron Microscopy, Atomic Force Microscopy are presented. Micromechanical properties measured during microindentation, scratch and wear tests are also shown.

Key words: boron nitride, pulsed laser deposition, coatings, nano-composites.

1. Introduction

Boron nitride (BN) is a chemical compound which is isoelectronic and isostructural with carbon. BN phases can be divided according to the bond hybridization into: sp^2-types i.e. a hexagonal h-BN, turbostratic t-BN and rhombohedral r-BN phases, with the structure and properties close to graphite, and sp^3-types – cubic c-BN and wurtzite w-BN forms, similar to diamond and lonsdaleite, respectively. All types of BN are chemically inert and corrosion-resistant insulators but good thermal conductors. Moreover, h-BN and r-BN phases are very soft, characterized by lubricating abilities similar to graphite. The cubic c-BN phase is characterized by high hardness, good abrasion resistance, high melting point and oxidation resistance at higher temperature, and practically no reactivity with iron group metals. The properties of w-BN are very close to the c-BN ones. Layers with c-BN or w-BN can be used as abrasion resistant tribological coatings as well as corrosion resistant ones protecting construction elements against chemically-aggressive environments and high temperature. They may also work as semiconducting layers. The h-BN and r-BN coatings can be used as anti-corrosion coatings and lubricating layers. Both sp^3- and sp^2-type phases may be applied as composites combining advantages of both soft and hard phases [1, 2].

This work is aimed at obtaining of nano-composite coatings based on BN-type phases, which could be used for special purposes as a lubricating tribological layer.

2. Experimental

Boron nitride thin films were obtained by ablation of the commercial h-BN target by means of a PLD deposition system. Two types of PLD apparatus were used:

1. The Nd:YAG laser with Q-switch operating in pulse mode (wavelength λ = 1064 nm, pulse duration τ = 10 ns, frequency f = 10 Hz, beam energy E = 0,6 J) was applied. Deposition was performed in an atmosphere of nitrogen, argon or in a mixture of nitrogen and argon. Austenitic steel or ferritic-austenitic steel substrates were unheated (T_S = 20°C) or heated (T_S = 400°C) during the process. Before BN deposition, samples had been covered with titanium buffer layer in the same PLD system. Samples were examined by X-ray diffraction (Philips PW 1830) and scanning electron microcopy (Philips XL30 and FEI XL30 E-SEM).

2. The KrF excimer laser (wavelength λ = 248 nm, pulse duration τ = 20 ns, frequency f = 6–20 Hz) was used for deposition of BN in nitrogen atmosphere on Ti6Al4V alloy without buffer layers or with titanium nitride interlayers obtained by glow discharge nitriding. An RF discharge generator (13.56 MHz, 100 W) was used to increase the gas ionization in the chamber and provide the deposited particles with higher energy. The RF field was generated parallel to the substrate, which was conditioned by the apparatus construction. In the case of Ti6Al4V alloy covered with Ti_xN layers substrates, an additional BN buffer layer was applied. It was obtained by the deposition of BN without RF generator (Table 1). Next, BN layers were deposited by PLD together with RF generator discharges. The PLD process was carried out at variable fluence (F = 5 J/cm^2 or 14 J/cm^2), as well as substrate temperature (T_S = 20; 500; 700°C) and nitrogen pressure (p = 5; 20 Pa). The samples were examined by Atomic Force Microscopy (Veeco Multi-Mode AFM Nanoscope IIIa), Fourier Transformed Infrared Spectroscopy (Perkin Elmer Spectrum GX) and Transmission Electron Microscopy (Philips CM20 and JEM 4000 EX). Mechanical properties were measured using Micro Combi Tester

*e-mail: nmmajor@imim-pan.krakow.pl

apparatus. Conditions of examinations of Vickers microhardness, scratch and wear tests are summarized in Tables 2–4.

Table 1
Deposition conditions of BN/Ti_xN/Ti6Al4V samples (constant deposition parameters are nitrogen pressure of 5 Pa and laser fluence of 14 J/cm^2)

Sample	Substrate temperature (°C)	Deposition of BN without working of RF generator so called "BN buffer"/number of laser pulses	Deposition of BN with working of RF generator/ number of laser pulses
BN11	700	no	yes / 20 000
BN12	700	yes / 5 000	yes / 10 000
BN13	500	yes / 5 000	yes / 10 000
BN14	500	no	yes / 20 000
BN15	20	yes / 5 000	yes / 10 000

Table 2
Conditions of microhardness measurement

Indenter	Diamond, Vickers type
Maximum load F_{max} (mN)	F_{max} = 20, LR = 40, UR = 40
	F_{max} = 50, LR = 100, UR = 100
Loading rate LR, unloading rate UR (mN/min)	F_{max} = 100, LR = 200, UR = 200
	F_{max} = 1000, LR = 2000, UR = 2000

Table 3
Conditions of scratch test

Scratch tip	Rockwell diamond C
Progressive linear load F (N)	0.03–30
Tip radius (μm)	200
Scratch length (mm)	2
Tip movement rate (mm/min)	2

Table 4
Conditions of "ball-on-disk" wear test

Ball	Corundum (90% Al_2O_3 + 4.5% SiO_2 + 5.5% others elements)
Radius of friction (mm)	2.5
Ball diameter (mm)	1
Rotational rate (rpm)	60
Number of cycles	2000
Load F (N)	1

3. Results

3.1. BN coatings obtained on steel with titanium buffer layers by means of pulsed Nd:YAG laser. The samples obtained on steel with titanium buffer layers are composed of nanocrystalline h-BN phase with average diameter of crystallites between 80 to 105 nm, which was determined on the basis of X-ray diffraction measurements. The thickness of the coatings measured by profilometer was of the order of a few hundred nanometers. The sample surface consists of uniformly distributed flake-like grains of h-BN with the maximum diameter of a few micrometers. There are many voids between the flakes, so the layers do not exhibit high packing density. There are almost no droplets on the surface. The morphology of the layers is homogenous in the whole area of the surface. SEM examinations of partially removed coatings showed that flake-like structure is kept up under the surface in the cross section of the layers. The morphology is very homogenous, irrespective of substrate temperature (Fig. 1), gas atmosphere or plasma plume energy. Texture analysis reveals that (0002) h-BN lattice planes are oriented parallel to the surface (Fig. 2), what remains in a good agreement with literature data where such [0002] out-of-plane orientation was observed in the case of deposition without additional substrate bias or ion bombardment [1].

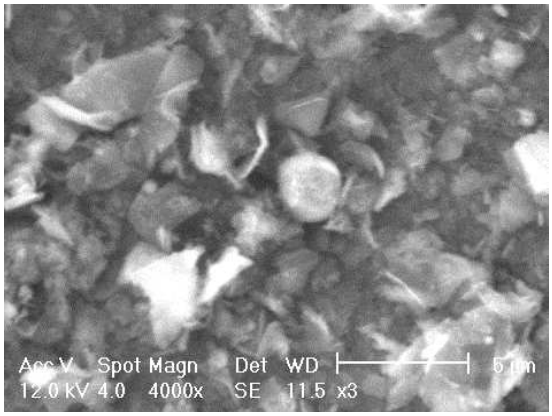

$T_S = 20°C$

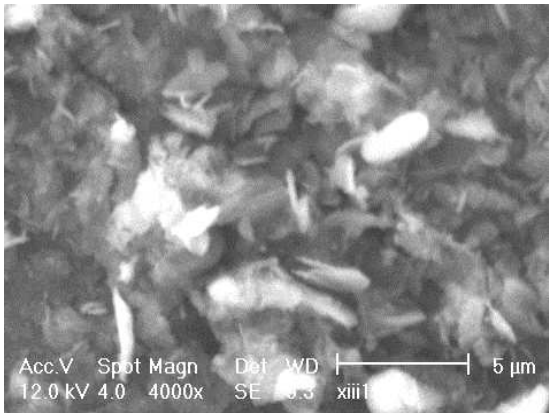

$T_S = 400°C$

Fig. 1. Surface images (SEM) of BN/Ti/ferritic-austenitic steel samples, obtained without sample heating (T_S = 20°C) as well as at elevated substrate temperature (T_S = 400°C)

3.2. BN layers obtained on Ti6Al4V substrate without any buffer layers by pulsed excimer KrF laser. The coatings obtained by ablation of h-BN on Ti6Al4V alloy without buffer layers are 380 to 850 nm thick and they did not undergo delamination. The layer thickness increases together with the decrease of nitrogen pressure and the raise of the substrate tem-

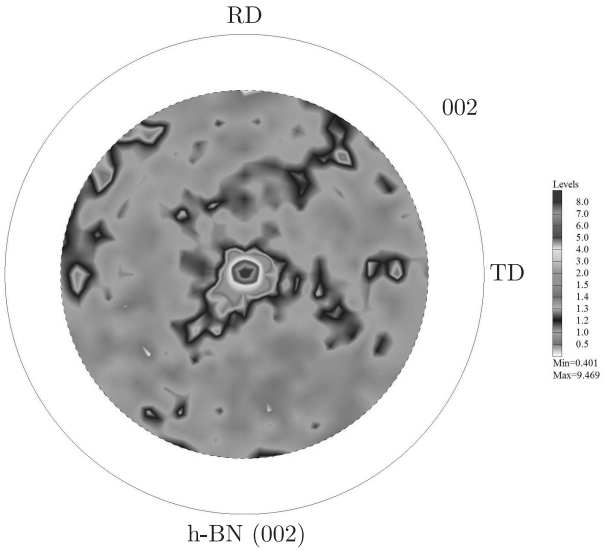

Fig. 2. Pole figure of (0002) h-BN planes in BN layer in BN/Ti/ferritic-austenitic steel sample obtained at 400°C

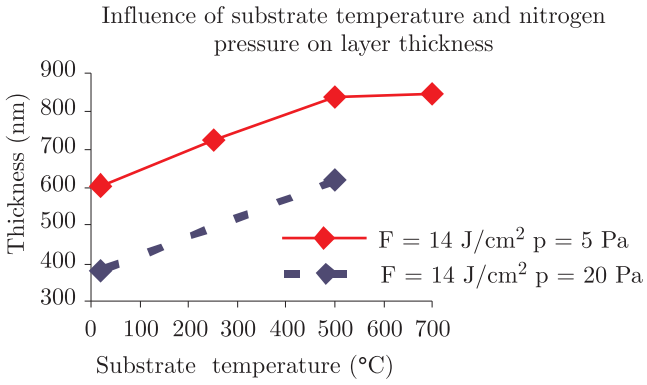

Fig. 3. Influence of substrate temperature and nitrogen pressure (p) on the thickness of BN layer deposited on Ti6Al4V substrates at the fluence of 14 J/cm^2

perature up to 500°C in specimens prepared at fluence of 14 J/cm^2 (Fig. 3). The quality of the coating surface is one of the most important parameters, decisive for its usability. Therefore the contribution of laser fluence to surface topography is examined. Figure 4 shows the surface morphology of BN/Ti6Al4V samples obtained at the same substrate temperature of 500°C, nitrogen pressure of 5 Pa and at various fluence of 5 or 14 J/cm^2. The growth rate of BN layer deposited at the fluence of 5 J/cm^2 (0.024 nm/pulse) was two times lower than in the case of the higher fluence of 14 J/cm^2 (0.056 nm/pulse). This proves that the number of effectively deposited particles strongly depended on laser beam energy density. The higher fluence was, the more BN particles were deposited on the substrate. The obtained structure is composed of fine-grained matrix and half-spherical-shaped conglomerates, consisting of columnar crystallites with semi-circular cross-section. The RMS roughness of 10×10 μm surface area is 67 nm and 186 nm in the case of high and low fluence, respectively. The application of laser energy density of 14 J/cm^2 produced thicker and smoother layers in comparison with that obtained at 5 J/cm^2. The surface profiles measured along the marked lines (Fig. 4) across the area with the largest clusters show, that conglomerates are even two times larger in diameter and relative height in the case of sample deposited at lower fluence than in sample obtained at the higher one. In that sample (F = 5 J/cm^2) crystallites are larger and much better shaped. This is probably due to the fact that the layer was obtained with lower growth rate when the amount of BN material delivered to the surface was smaller and incoming atoms have had more time to migrate into more thermodynamically stable positions before they were coated by the next portion of material [12–14]. The morphology of the same sample varies with the lateral position. It might be related to the fact, that laser-induced plasma plume has non-uniform shape, described by the mathematical function proportional to $\cos^n\varphi$. The sample obtained without substrate heating and at the fluence of 14 J/cm^2 is examined in the central and near-edge area regions. The peripheral position resulted in a lower deposition rate, as compared with the one in the central part. Layers grew slower near the edges of the sample and therefore crystallites are larger and have smoother surfaces, while in the central part of the sample, they are a few times smaller with accumulation of deposited material in the crystallite boundaries. It is possible that layer started to grow rather in direction parallel to the substrate surface and an accumulation of deposited material may be the effect of the coalescence of approaching crystallites.

3.3. BN layers obtained on Ti6Al4V substrate with titanium nitride buffer layers by pulsed excimer KrF laser. The phase composition was analyzed by means of Fourier Transform Infrared Spectroscopy (FTIR) measurements in reflective mode. Figure 5 presents the spectra of the samples obtained without substrate heating or at 500°C as well as at 700°C, and the spectrum of the nitrided Ti6Al4V substrate. The spectrum of the sample deposited at the highest substrate temperature (T_S = 700°C) is characterized by strong absorptive peaks at the frequencies of about 780 and 1340 cm^{-1}, characteristic for bond vibrations in h-BN particle, which appear at 780 and 1320–1400 cm^{-1} [1,3–5]. The maximum of peak of the tensile vibrations of B-N bond is observed to be shifted towards lower frequencies (the peak appears at 1370 cm^{-1} in the reference h-BN crystal). This suggests that there is tensile stress in the BN layer [3]. Such stress could improve the overall layer adhesion by compensating compressive stress, usually encountered in the areas with the sp^3-type phase obtained by PLD method and frequently responsible for layer delamination. The spectrum obtained from the layer produced at 500°C is characterized by a considerably reduced intensity of the signals received from the sp^2-BN form and contains only a small intensity peak with the maximum at about 1350 cm^{-1}. This could have been caused by the decrease of amount of crystalline h-BN and t-BN and the tendency of amorphous BN (a-BN) to increase its share in the entire layer volume. No clear signals originating in h-BN are visible in the spectrum of the coating deposited without substrate heating. The fluctuations of the FTIR 700°C line around 1100–1120 cm^{-1} are most probably related to the superposition of a small peak with the

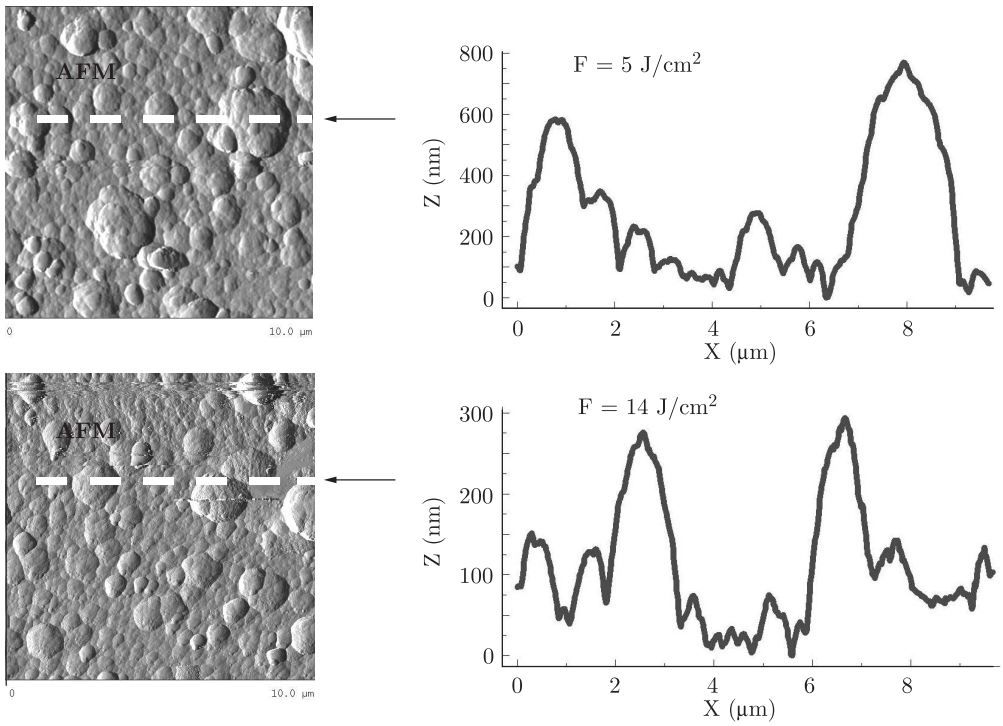

Fig. 4. AFM images (area 10×10 μm) and roughness profiles of the surface of BN/Ti6Al4V samples obtained at various fluence namely 5 J/cm^2 and 14 J/cm^2

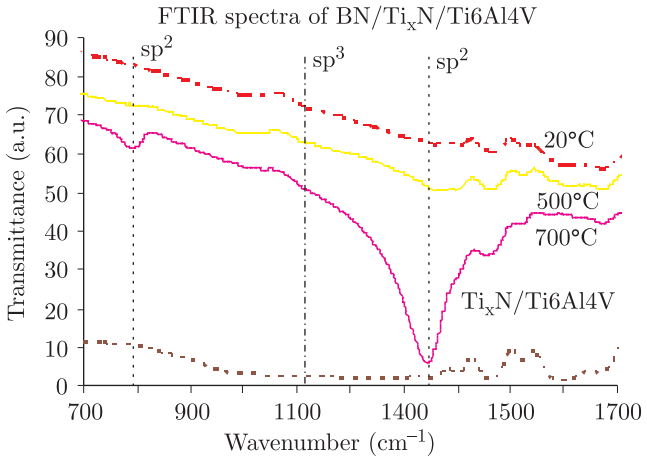

Fig. 5. FTIR spectra of BN coatings deposited at the fluence of 14 J/cm^2 and nitrogen pressure of 5 Pa and at various substrate temperatures (T_S = 20, 500 and 700°C) on nitrided Ti6Al4V alloy

band originating in the sp^2-phase (Fig. 5). Such frequency value corresponds to the reference data originating in c-BN (1065–1100 cm^{-1} [1,5,6]) or w-BN (1090, 1120 and 1230 cm^{-1} [1]). The peak visible at the band slope ascribed to h-BN can originate in the peaks at 1090 and 1120 cm^{-1}, which suggests, together with HRTEM data, the w-BN phase presence.

The surface morphology changes strongly with the substrate temperature (Fig. 6). The increase of the substrate temperature from 20 to 700°C led to the formation of better shaped and larger crystallites and decreased the amount of amorphous-like material, which covers the whole surface in the case of 20°C, while it is localized only in crystallites boundaries in the sample obtained at 700°C. Such observations correspond to FTIR results and suggest that the raise of the substrate temperature caused the change of matrix composition from mostly amorphous at 20°C to highly crystalline sp^2-BN at 700°C.

Table 5
Interplanar distances of the BN layer deposited at 700°C on Ti6Al4V alloy with titanium nitride buffer layers at the fluence of 14 J/cm^2 and nitrogen pressure of 5 Pa, measured in HRTEM cross-sectional image

Experimental interplanar distance (nm)	(hkl) plane phase	Reference interplanar distance (nm)
0.33–0.35 ± 0.01	(0002) h-BN	0.330
	(0002) t-BN	0.350–0.380
0.19–0.20 ± 0.01	(101) w-BN	0.196
0.22–0.23 ± 0.01	(100) w-BN	0.221

Thickness of the deposited BN layers measured on the TEM micrographs of the cross-section foils varies in the range from 100 to 400 nm. The thickness increases with the raise of the substrate temperature. Electron diffraction patterns taken from glow discharge nitrided buffer area of Ti6Al4V alloy revealed existence of layered structure composed of Ti_2N phase in the deeper region and TiN in the area adhering directly to BN. Crystalline structure of BN is dominant in BN12 sample while amorphous in BN15 sample. The TEM microstructure of the sample obtained at 700°C is presented in Fig. 7. HRTEM examinations showed that a BN layer with nano-composite

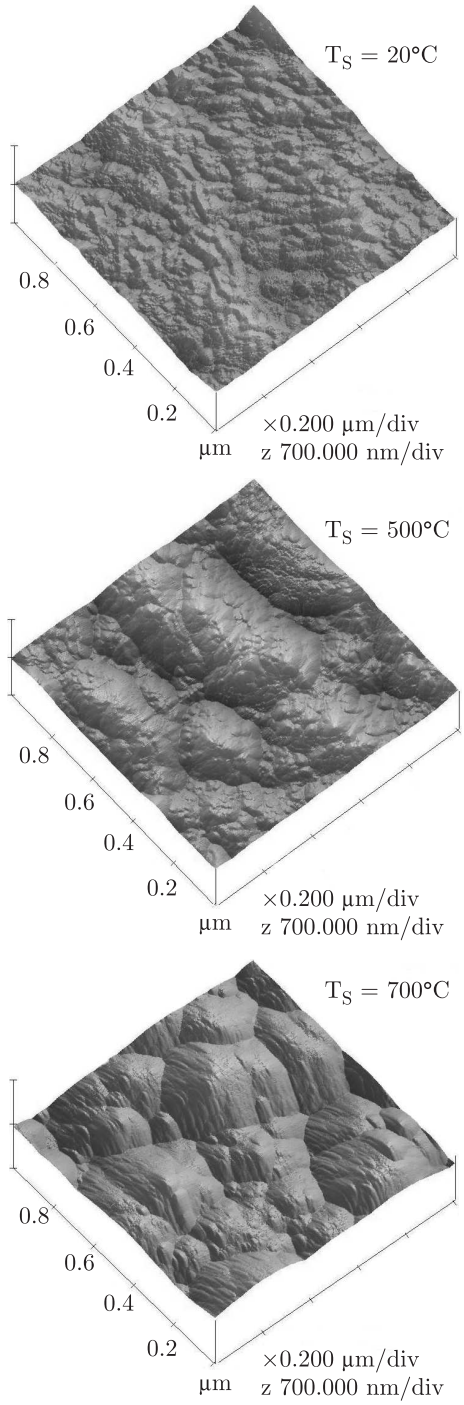

Fig. 6. AFM images (area 1×1 µm) of the surface of the samples obtained on nitrided Ti6Al4V alloy at substrate temperature of 20°C, 500°C or 700°C and with the fluence of 14 J/cm^2 and nitrogen pressure of 5 Pa

structure is obtained. The matrix is built of the graphite-like soft phase of the sp^2-type, consisting primarily of t-BN and h-BN. It is not strongly texturized with (0002) planes perpendicular to the substrate, contrary to the examples described in the relevant literature [1,8–10]. Particles 5–10 nm in diameter are built into the matrix. In some cases, the particles reach the diameter of 20–50 nm. The analysis of the distances between atomic planes of crystallites indicates the existence of w-BN phase (Table 5). Similar results were obtained by Hu et al. for the layers deposited by radio frequency sputtering [7]. Figure 8 presents HRTEM image of a single w-BN crystallite. It seems that the absence of characteristic laminar sequence (a-BN/sp^2-BN/sp^3-BN) – often presented in the relevant literature for coatings consisting of h-BN and c-BN [1,8–10] – is due to the fact that w-BN form is obtained. The mechanism of transformation of h-BN into w-BN is different than in the case of the transformation into c-BN. The creation of the w-BN phase is thermodynamically more favourable, because it requires less energy as the crystalline structures of both phases are similar (the same sequence of layers and lattice symmetry) and can proceed as a result of direct diffusionless h-BN → w-BN phase transformation [11].

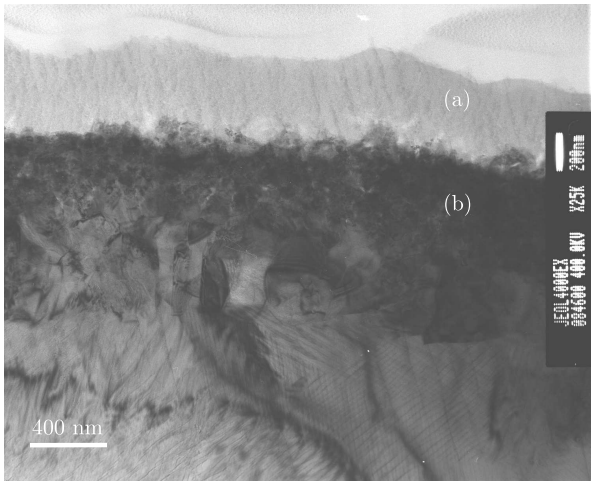

Fig. 7. TEM microstructure of the cross-section of the BN layer deposited at 700°C at the fluence of 14 J/cm^2 and nitrogen pressure of 5 Pa on Ti6Al4V alloy with titanium nitride buffer layers: BN (a), TiN (b)

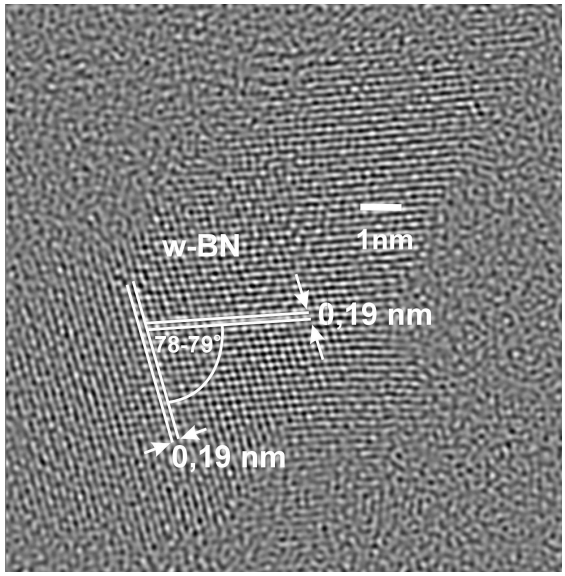

Fig. 8. HRTEM microstructure of crystallite in the BN layer obtained at 700°C on nitrided Ti6Al4V at the fluence of 14 J/cm^2 and nitrogen pressure of 5 Pa

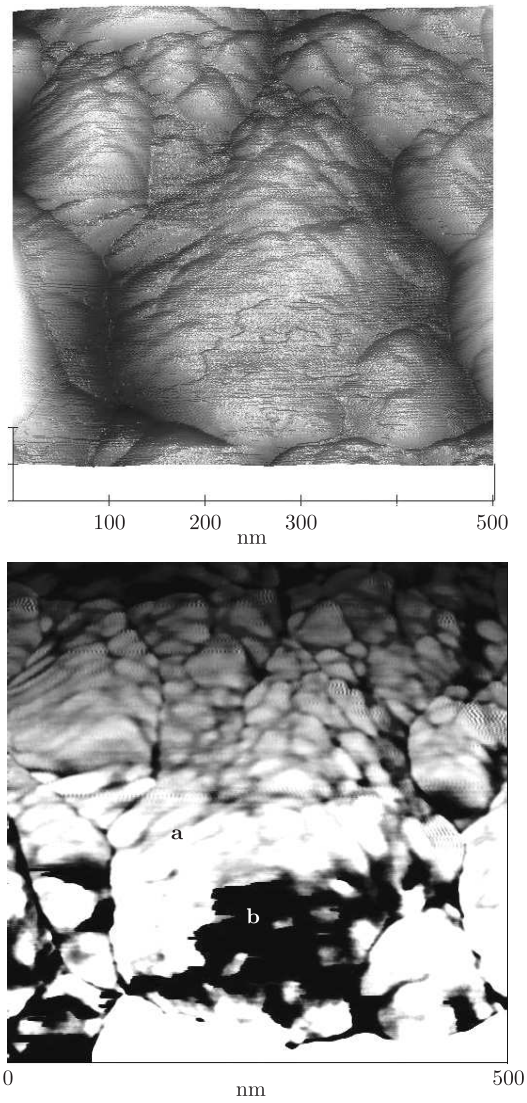

Fig. 9. AFM images of surface of BN12 sample. Left – topography image collected in tapping mode. Right – image obtained in Phase Imaging Mode with areas (white (a) and black (b)) characterized by different character of interactions between sample surface and AFM tip during imaging process

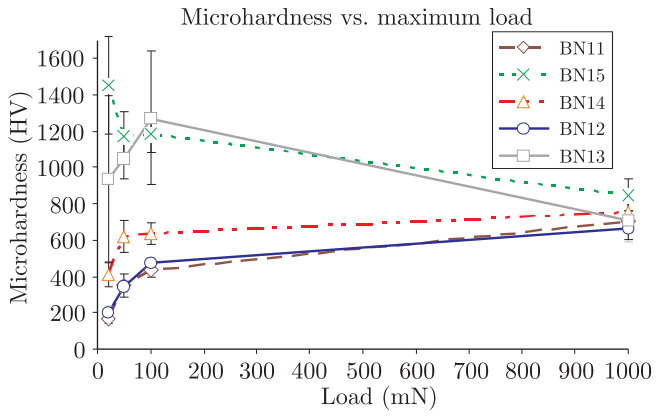

Fig. 10. Dependence of hardness from maximum applied load obtained during Vickers indentation test of BN/Ti$_x$N/Ti6Al4V specimens

Table 6
Mechanical properties of BN/Ti$_x$N/Ti6Al4V samples (F – maximum load, HV – microhardness, δHV – standard deviation of microhardness h – maximum indentation depth, δh – standard deviation of maximum indentation depth, E – Young's modulus, δE – standard deviation of Young's modulus)

Sample	F (mN)	HV (a.u.)	δHV (a.u.)	h (nm)	δh (nm)	E (GPa)	δE (GPa)
BN11	20	170	26	651	48	77.3	6.1
	50	353	64	737	70	107.5	8.0
	100	438	42	952	55	138.0	12.2
	1000	703	60	2569	93	139.7	13.6
BN12	20	204	34	610	43	93.9	7.6
	50	345	30	742	31	129.6	5.3
	100	474	25	919	26	138.5	13.2
	1000	664	70	2630	99	135.3	14.0
BN13	20	939	454	335	81	182.9	40.5
	50	1048	108	436	15	231.3	23.2
	100	1271	368	612	64	228.2	32.6
	1000	712	104	2581	156	132.7	8.7
BN14	20	408	65	426	39	125.9	9.9
	50	621	87	555	35	159.0	19.3
	100	640	58	797	38	184.4	16.0
	1000	758	71	2533	104	134.4	7.1
BN15	20	1453	268	247	26	220.4	19.9
	50	1172	139	430	16	201.7	8.1
	100	1188	107	612	21	203.5	13.5
	1000	850	86	2436	101	137.0	9.6

3.4. Mechanical properties of BN/Ti$_x$N/Ti6Al4V specimens. Specimens of BN/Ti$_x$N/Ti6Al4V were examined on Micro Combi Tester (MCT CSEM) apparatus. Vickers microhardness (HV) and Young's modulus (E) together with maximum load (F) and indentation depth (h) are presented in Table 6. HV results measured at load of 20 mN are between 170 to 1453 HV depending on specimen. The lowest hardness is observed in samples which possess the thickest BN layer and the highest degree of crystalline sp^2-BN, i.e. BN12 and BN11. The highest hardness of BN15 sample must be connected with the fact, that there is only a very thin amorphous layer of BN which should be very soft and total microhardness value originates mainly from hard sublayers of TiN and Ti$_2$N. Analysis of displacement-load curves of BN11 and BN12 samples reveals existence of a very soft top layer which have a thickness of about 400–500 nm. This is in a good agreement with TEM results showing a 400 nm layer of BN on the top of TiN layer. Standard deviation of BN12 average microhardness obtained at the load of 20 mN is 34 HV which is about 17% of the value. Results of other samples BN13, BN14 and BN15 are characterized by even larger standard deviation reaching 48% of the value in the case of sample BN13. It means that the surface is non homogenous but there are softer and harder areas, probably containing various phases. This is confirmed in AFM Phase Imaging Mode images of sample BN12 (Fig. 9). Two distinct areas which are observed result from different interactions of AFM tip with the sample surface. The "white" and the "black" fields in the image mean that there are areas

with different crystallinity, adhesion etc. which influenced on contrast in Phase Detection Mode. These areas may have different hardness. Microhardness value changes with increasing load and indentation depth. microhardness progressively rises in the case of samples BN11, BN12 and BN14, while lowers continuously in BN15. In BN13 sample, first, raises up to 1271 HV at 100 mN of load and than decreases (Fig. 10). Microhardness values of all samples measured at the load of 1000 mN are about 700–850 HV. The evolution of Young's modulus (E) is shown in Fig. 11. At the lowest load of 20 mN Young's modulus values are from 77.3 GPa (BN11) to 220.4 GPa (BN15). At the load of 1000 mN, in each sample Young's modulus reaches value of 135–140 GPa and penetration depth about 2500 nm.

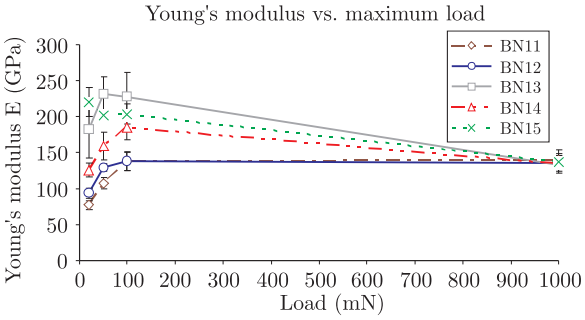

Fig. 11. Dependence of Young's modulus from applied load obtained during Vickers indentation test of BN/Ti_xN/Ti6Al4V specimens

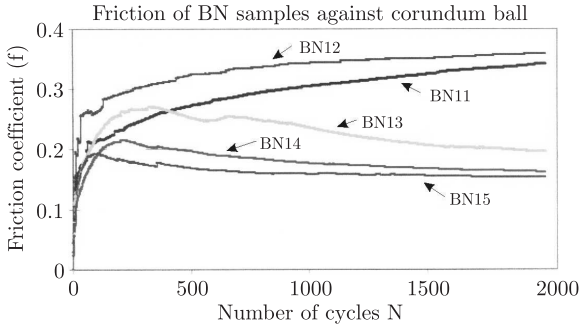

Fig. 12. Dependence of friction coefficient from number of cycles obtained during "ball-on-disk" wear test of BN/Ti_xN/Ti6Al4V specimens

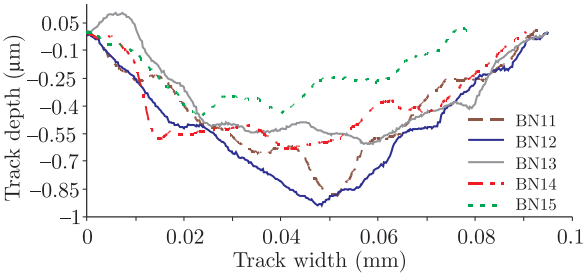

Fig. 13. Profiles of wear tracks of BN/Ti_xN/Ti6Al4V samples obtained during "ball-on-disk" wear test

The scratch tests performed with Rockwell diamond tip reveals no brittle cracking of the surface. In BN11, BN12 and BN13 samples, according to optical microscopy observations, there are no exposing of the Ti6Al4V substrate even after applying the maximum force of 30 N. BN surface layer causes a decrease of friction coefficient. Increase in this coefficient takes place after reaching the penetration depth of 2–3 micrometers when the indenter fall into contact with Ti_xN layers. In other two samples, according to optical microscopy observations, uncovering of the substrate is visible at the load of 26.7 N and depth of 21.7 μm as well as at load of 18.4 N and depth of 16.8 μm, for BN14 and BN15, respectively. A friction coefficient of the samples progressively rises up to 0.16, except of sample BN15 which reaches the value of 0.2.

Dry sliding wear tests of samples against alumina ball were carried out. During tests a friction coefficient was continuously recorded. Dependence of a friction coefficient from number of sliding cycles is presented in Fig. 12. The graph shows an evolution of friction coefficient. In all samples two stages are clearly visible. Step 1, up to 100–200 cycles, is attributed to matching and smoothing of the sliding surfaces. Progressive raise of friction coefficient up to f = 0.2–0.3 is observed. In the second step friction coefficient is reduced to a constant value in samples BN13 (f = 0.2), BN14 (f = 0.18) and BN15 (f = 0.16). The other samples, i.e. BN11 and BN12, reveal a proportional raise of friction coefficient to value of around 0.35. After 2000 cycles, at the end of the tests, the lowest friction coefficient is observed in BN15 (f = 0.16), while the highest in BN12 (f = 0.36) sample. It seems that applying of lower substrate temperature during BN deposition, which led to obtaining of thinner and less crystalline BN layer, allows to decrease the friction coefficient. According to AFM examinations (Fig. 6) the surface morphology and roughness of BN12 and BN15 samples are different what may also influence the friction behaviour. Cross-sectional profiles of wear tracks are presented in Fig. 13, while their cross-sectional areas are shown in Fig. 14. The largest wear depth is observed in samples BN11 and BN12, 890 and 940 nm, respectively. In these samples BN was deposited at the highest temperature of 700°C with the largest thickness of the BN layer of around 400 nm and high degree of crystalline sp^2-BN. BN13 and BN14 samples have a wear depth around 600 nm, while BN15 is characterized by the smallest value of 450 nm. In all cases, wear depth is larger than a thickness of BN layers deposited on the surface of Ti_xN/Ti6Al4V specimens. Therefore BN layers must have been removed during sliding but they could also act as a lubricant layer forming a thin layer between the sample surface and the corundum ball leading to decrease of measured friction coefficient. A total cross-sectional area of wear track depends on the temperature of BN deposition (Fig. 14). The largest area is in the case of BN12 and BN11, while the lowest in BN15 sample. Wear depths and areas are very close in BN11 and BN12 as well as BN13 and BN14 what indicates that applying of "buffer BN" does not influence the wear behaviour in this test. In general, samples show good wear resistance and low friction coefficient. In this test BN15 exhibits the best wear resistance of all samples, what is contrary to the results of scratch test. Differences may result from various material and geometry of scratch tip and wear ball. More tribological tests are being made.

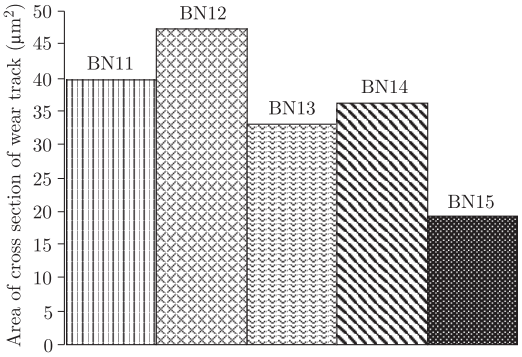

Fig. 14. Area of cross section of wear tracks obtained during "ball-on-disk" wear test of BN/Ti_xN/Ti6Al4V specimens

4. Concluding remarks

The morphology and composition of deposited BN layers depends on the type of laser. The Nd:YAG laser allowed to obtain h-BN coating with flake-shaped grains. The layers are nanocrystalline and strongly texturized. The deposition parameters have no visible influence on the surface morphology or phase constitution.

The surface morphology of BN layers obtained by KrF laser on Ti6Al4V substrate without any buffer layers depends on the process parameters. The surface consists of the fine-grained matrix and the half-spherical-shaped conglomerates. Lower fluence results in the formation of larger and better-formed crystallites and increases the roughness, which is probably caused by the fact that the amount of material arriving at the lower fluence to the surface was smaller and the incoming atoms had more time to migrate into thermodynamically stable positions. The morphology of the same sample varies in the lateral position. The layers grew slower near the edges of the sample and therefore the crystallites are larger and have smoother surfaces. In the central part of the sample, the crystallites are a few times smaller with accumulation of deposited material in the grain boundaries.

The deposition of BN layers by KrF laser and enhanced by the RF generator at 700°C on glow discharged nitrided Ti6Al4V alloy substrate led to layers with nano-composite structure. The sample consists of a w-BN phase particles located in a t-BN and h-BN matrix on the top of Ti_xN/Ti6Al4V substrate. Decreasing the substrate temperature to 20°C caused decrease of amount of crystalline sp^2-phase. The lowest Vickers microhardness is observed at the indentation load of 20 mN for samples obtained at 700°C, which have 400 nm layer of crystalline BN layer. Results are a superposition of values resulting from BN and Ti_xN layers. Surface of samples is rather non homogenous, it seems that it consists of areas with different microhardness. Young's modulus is 77–220 GPa in the case of 20 mN load and 135-140 GPa at 1000 mN of load. Scratch tests reveal no brittle cracking of the surface. In samples obtained at 500°C without "BN buffer" and at 20°C with "BN buffer" Ti6Al4V substrate was uncovered at load of 26.7 N and 16.8 N, respectively. Other samples did not reveal uncovering of the substrate. Dry sliding wear tests of the surface against corundum ball reveals small wear with the depth less then one micrometer. The highest wear resistance has a sample with BN deposited at 20°C while the lowest sample with BN obtained at 700°C. In general, multilayer systems BN/Ti_xN/Ti6Al4V are composed of soft BN outer layer on hard Ti_xN layers. These systems are characterized by low friction coefficient and good wear resistance during dry sliding wear tests.

Acknowledgements. The research was financed from PBZ-KBN-100/T08/2003 project and from the means provided by the Polish Ministry of Science and Informatization, within the Program: "Development of systems for innovative solutions in production and operation in 2004-2008" as well as by the Knowledge-based Multicomponent Materials for Durable and Safe Performance KMM NoE project.

REFERENCES

[1] P.B. Mirkarimi, K.F. McCarty, and D.L. Medlin, "Review of advances in cubic boron nitride film synthesis", *Materials Science and Engineering* R21, 47–100 (1997).

[2] R. Haubner, M. Wilhelm, R. Weissenbacher, and B. Lux, "Boron nitrides properties synthesis and applications", *Structure and Bonding* 102, 1 (2002).

[3] Y. Yap, T. Aoyama, Y. Wada, M. Yoshimura, Y. Mori, and T. Sasaki, "Growth of adhesive c-BN films on a tensile BN buffer layer", *Diamonds and Related Materials* 9, 592–595 (2000).

[4] C. Ronning, H. Feldermann, and H. Hofsass, "Growth, doping and applications of cubic boron nitride thin films", *Diamonds and Related Materials* 9, 1767– 1773 (2000).

[5] A. Klett, R. Freudenstein, M.F. Plass, W. Kulisch, "Stress of c-BN thin films: a parameter investigation", *Surface and Coatings Technology* 116–119, 86–92 (1999).

[6] S. Acquaviva, G. Leggieri, A. Luches, A. Perrone, A. Zocco, N. Laidani, G. Speranza, and M. Anderle, "Cubic boron nitride deposition on silicon substrates at room temperature by KrF excimer laser ablation of h-BN", *Applied Physics* A70, 197–201 (2000).

[7] C. Hu, S. Kotake, Y. Suzuki, and M. Senoo, "Boron nitride thin films synthesized by reactive sputtering", *Vacuum* 59, 748–754 (2000).

[8] S. Weissmantel and G. Reisse, "Properties of ion-assisted PLD h-BN/c-BN layer systems", *Applied Surface Science* 154–155, 428– 433 (2000).

[9] G. Reisse and S. Weissmantel "Characterization of pulsed laser deposited h-BN films and h-BN/c-BN layer systems", *Thin Solid Films* 355–356, 105–111 (1999).

[10] D. Kester, K. Ailey, D. Lichtenwalner and R. Davis, "Growth and characterization of cubic boron nitride thin films", *Journal of Vacuum Technology* A12 (6), 3074 (1994).

[11] T. Sekine, Sato, "Shock-induced mechanisms of phase transformations from rhombohedral BN to cubic BN", *Journal of Applied Physics* 74(4), 2440– 2444 (1993).

[12] J. E. Greene, "Physics of film growth from the vapor phase", in *Multicomponent and Multilayered Thin Films for Advanced Microtechnologies: Techniques, Fundamentals and Devices*, eds. O. Auciello, J. Engemann, Kluwer Academic Publishers, NATO ASI Series E: *Applied Sciences* 234, 39 (1993).

[13] G.H. Gilmer, H. Huang, and C. Roland, "Thin film deposition: fundamentals and modelling", *Comp. Mat. Sc.* 12, 354–380 (1998).

[14] W. Mróz, "Physics of growth of thin films deposited by laser ablation", E-MRS 2003 Fall Meeting, *Solid State Phenomena* 101–102, 187–196 (2005).